Effects of meson-decay diagrams in proton-proton bremsstrahlung

F. de Jong[1-3] and K. Nakayama[1,2]

[1]*Department of Physics and Astronomy, University of Georgia, Athens, Georgia 30602*
[2]*Institut für Kernphysik, Forschungszentrum Jülich, 52428 Germany*
[3]*Kernfysisch Versneller Instituut, 9747 AA Groningen, The Netherlands*

We investigate the effect of meson-decay diagrams on the proton-proton bremsstrahlung process. We explicitly include short-range correlations by calculating single- and double-scattering diagrams using an NN T-matrix interaction. We find that in general these diagrams interfere destructively with the corresponding Born amplitudes so that the net effect of the meson-decay process on proton-proton bremsstrahlung reactions is considerably smaller than that of the Born amplitude alone.

I. INTRODUCTION

Triggered by the availability of new data [1,2] a series of theoretical studies of the proton-proton bremsstrahlung ($pp\gamma$) process have appeared in the past few years [3–9]. Compared to older work, these studies are based on modern realistic NN interactions, and incorporate higher order terms in the photon momentum, like the rescattering contribution and relativistic spin correction. These new calculations all show one remarkable feature: The contributions from the nuclear current are insensitive to the specific NN potential employed once the NN phase shifts are reproduced. As has been pointed out in Refs. [10,11], this is basically due to the fact that the $pp\gamma$ reaction is insensitive to the spin-singlet component of the NN interaction in which the largest off-shell differences are present among modern realistic interactions. In the spin-triplet components (especially the tensor component) to which the $pp\gamma$ reaction is most sensitive, these interactions have a rather similar off-shell behavior in regions sampled by the $pp\gamma$ process. This is unfortunate for the pp bremsstrahlung program as a tool for measuring the half-off-shell behavior of the NN interaction. On the other hand, however, this insensitivity to the particular NN interaction allows us to investigate the reaction mechanism of $NN\gamma$ processes due to higher order corrections, especially those due to two-body currents such as the Δ-isobar decay, heavy isoscalar meson exchange currents, etc. For example, in contrast to the elementary $np\gamma$ or deuteron photo- and electrodesintegration processes, where there is a cancellation between the different Δ decay diagrams involved due to isospin factors, the $pp\gamma$ reaction is more sensitive to this subnucleonic degree of freedom because of the absence of such a cancellation. Also, the $pp\gamma$ reaction is more suited for studying the role of isoscalar meson exchange currents than the $np\gamma$ process or photo- and electrodesintegration of the deuteron; the $pp\gamma$ reaction filters out the (otherwise dominant) pion- and rho-exchange currents.

The study of these higher order processes in connection with the $pp\gamma$ reaction has been taken up recently, although there are some earlier efforts in this direction [12–15]. In Refs. [16,17] we presented a calculation of the effects of Δ degrees of freedom and found sizable effects on the observables, both below and above pion threshold. Δ degrees of

freedom enter in two ways: First, one has Δ intermediate states in the T matrix, and second, and most importantly, one has the Δ decay diagrams (i.e., diagrams with a $N\Delta\gamma$ vertex). Inclusion of Δ degrees of freedom is of special interest since it allows one to go up in laboratory energies to energies of 1 GeV. In the present work we investigate the role of the two-body current due to the vector-meson decay process. Our approach differs from the recent work of Jetter and Fearing [18] and Eden and Gari [19] in that we take into account the single- as well as the double-scattering (or rescattering) contributions in addition to the Born contribution. In Refs. [18,19] the meson-decay as well as the Δ-decay diagrams are calculated in the Born approximation.

In Ref. [18] the authors account for the T matrix (or single-scattering and rescattering diagrams) effects of both the Δ-decay and meson-decay diagrams by introducing an energy-dependent renormalization factor. They fix the value of this factor by fitting their Δ-absorption cross section to the full T-matrix result of Ref. [20]. Judging from the results of Ref. [16], where the $pp\gamma$ reaction with both the Born and full T matrix was calculated, this simple renormalization seems, at least at low energies, a fair procedure for the Δ-decay diagrams. Note that the short-range correlation is much weaker for NN to $N\Delta$ scattering than for NN to NN scattering [21].

However, there are no certainties as to why the above renormalization procedure should be reasonable for the meson-decay diagrams. In their kinematics these diagrams look much more like the NN interaction itself. Since the short-range correlation plays a crucial role in the screening of the core of the bare NN interaction, one would expect a more pronounced effect of single-scattering and rescattering terms on the meson-decay diagrams. In this paper we will explicitly calculate these diagrams to investigate this question. First we will define our theoretical basis, and then we will point out how we implement these in our existing model of $pp\gamma$. Finally we will present results.

II. THEORETICAL FRAMEWORK

We first define our two-body current due to the meson-decay process. We will restrict ourselves to the $\omega\pi\gamma$-decay diagram since this diagram is the most important meson de-

cay diagram [18,19], following the dominant Δ-decay diagrams. We thus have the following vertices and propagators in defining the two-body current:

$$\Gamma^\mu_{\omega NN} = -ig_{\omega NN}\left(\frac{\Lambda^2_\omega + m^2_\omega}{\Lambda^2_\omega + \bar{q}^2}\right)\gamma^\mu,$$

$$\Gamma_{\pi NN} = g_{\pi NN}\left(\frac{\Lambda^2_\pi + m^2_\pi}{\Lambda^2_\pi + \bar{q}^2}\right)\gamma^5,$$

$$G^{\mu\nu}_\omega = \frac{g^{\mu\nu}}{\bar{q}^2 + m^2_\omega}, \quad G_\pi = \frac{-1}{\bar{q}^2 + m^2_\pi}, \quad (1)$$

with the numerical values $g^2_\pi/4\pi = 14.4$, $\Lambda_\pi = 1.7$ GeV, $m_\pi = 0.138$ GeV, $\Lambda_\omega = 1.5$ GeV, $m_\omega = 0.783$, and q is the momentum carried by the meson. The form factors in the meson-NN vertices as well as the values of the parameters quoted are the same as employed in the Bonn potential [22]. The omega NN coupling constant as used in the Bonn potential requires some consideration. Compared to the values typically found in pion photoproduction [25,26] and also from the broken SU(3) prediction of $(g_{NN\omega}/g_{NN\rho})^2 = 9$, the omega coupling constant of the Bonn potential is rather large. This is due to the fact that the omega coupling constant contains a lot of "effective" strength; i.e., apart from the "real" omega it simulates some of the processes which are not included in the model. Obviously the effective part of the strength has nothing to do with the omega decaying into a pion and photon. We thus think it is more realistic to adopt a value used in pion photoproduction: $g_{\omega NN} = 7.98$ [25,26]. This is about half the value used in the Bonn potential.

Of course, this choice, in conjunction with using other parameters of the nucleon-nucleon-meson vertices as they are used in the Bonn model, is somewhat arbitrary. For example, in the photoproduction calculation of Ref. [25] a cutoff is used to render the Born amplitudes (which are used as the driving term in the integral equation) square integrable. These authors use a monopole form factor with the cutoff parameter $\Lambda = 650$ MeV, which is much softer than the Bonn form factors. However, pion photoproduction is an s-channel process, whereas the diagrams we consider are t-channel processes and there is no straightforward way of relating these form factors in different channels.

The $\omega\pi\gamma$ vertex is (k is the outgoing photon momentum, and q is the outgoing pion momentum)

$$\Gamma^{\omega\pi\gamma}_{\nu\mu} = -ig_{\omega\pi\gamma}\epsilon_{\mu\alpha\gamma\nu}k^\alpha q^\gamma. \quad (2)$$

In this expression $\epsilon_{\mu\alpha\gamma\nu}$ is the totally antisymmetric Levi-Civita tensor; the index ν is to be contracted with the index of the omega propagator while the index μ is to be contracted with the index of the photon polarization. For $g_{\omega\pi\gamma}$ we take again the value from pion photoproduction, $g_{\omega\pi\gamma} = 2.71$ GeV^{-1} [25]. In Ref. [26] a value $g_{\omega\pi\gamma} = 2.26$ is used. Also note that this vertex (as all decay vertices) is gauge invariant by construction. Also, in leading order the contribution is of first order in the photon momentum.

Putting everything together we find, for our current (the momenta are defined in the initial NN c.m. frame),
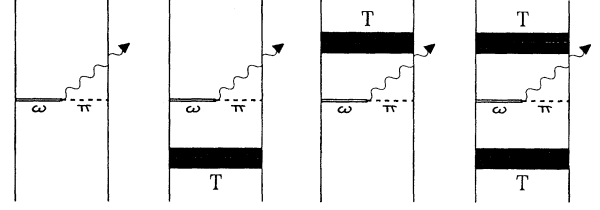
FIG. 1. The various diagrams with the $\omega\pi\gamma$ vertex we include in our model. The diagrams where the ω and π are interchanged are also included.

$$V^{\omega\pi\gamma}_{r'_1,r'_2,r_1,r_2}(p',p,k) = \left[\bar{u}_{r'_1}\left(\bar{p}' - \frac{\bar{k}}{2}\right)\Gamma^{\omega NN}_\mu u_{r_1}(\bar{p})\right]$$

$$\times G^{\mu\nu}_\omega\left(\bar{p}' - \frac{\bar{k}}{2} - \bar{p}\right)\Gamma^{\omega\pi\gamma}_{\kappa\nu}\epsilon^\kappa$$

$$\times G_\pi\left(-\bar{p}' - \frac{\bar{k}}{2} + \bar{p}\right)$$

$$\times \left[\bar{u}_{r'_2}\left(-\bar{p}' - \frac{\bar{k}}{2}\right)\Gamma^{\pi NN}u_{r_2}(-\bar{p})\right]. \quad (3)$$

In this equation ϵ^κ is the polarization of the photon, k is the photon momentum, and p and p' are the relative momenta of the incoming and outgoing nucleons, respectively. Some comments are in order here. For reasons of chiral invariance the pseudovector coupling is conventionally preferred over the pseudoscalar coupling for the πNN vertex. Using the full meson propagators these two couplings give the same result for the Born amplitude of our current. One might, however, expect differences to show up in the single-scattering and rescattering contributions. As we explicitly verified the differences between the results calculated with these two vertices are minor. By performing a calculation where we used the full four-momentum in the meson propagators in Eq. (3) we tested the effects of the static approximation of the meson propagators. Again we found only minor differences.

With all elements defined we only need to specify the diagrams we include in our calculation. The calculation of the contributions of the nucleonic current is described elsewhere [4,5]. It includes the rescattering contributions as well as the relativistic spin correction. The additional diagrams we now include are depicted in Fig. 1. Diagrams with the pion and ω meson interchanged are not displayed but are taken into account in the calculation. In the calculation at energies above the pion threshold Δ degrees of freedom become very important. We thus consider diagrams in which the pion couples to a $N\Delta$ vertex. We calculated the counterparts of Figs. 1(b),1(c) with a $N\Delta\pi$ vertex. It turned out that these only provided a minor contribution. For computational reasons we did not calculate the counterparts of Fig. 1(d), but since the other diagrams were small we do not expect that this diagram would give a sizable contribution.

For the NN interaction required in these diagrams we use the Bonn T matrix [22] for the calculations below pion threshold and a T matrix including Δ intermediate states [23,24] for the calculations above the pion threshold. The latter was also used in Ref. [17]. We thus have to employ the

underlying approximations of these T matrices, like the three-dimensional reduction of the intermediate momentum integration, the use of static meson propagators, and restricting intermediate states to positive energy states only. These are exactly the same approximations made in calculating the rescattering contributions from nucleonic currents.

In our formalism all contributions have a covariant normalization and we thus can calculate all diagrams in any convenient frame. For example, we evaluate diagram 1(d) in the initial c.m. frame. In this frame we have the following expression (the tilde denotes Lorentz-invariant matrix elements):

$$
\tilde{M}^{\omega\pi\gamma}_{r'_1,r'_2,r_1,r_2} = \int \frac{p''}{(2\pi)^3} \frac{p'''}{(2\pi)^3}
$$

$$
\times \sum_{r''_1,r''_2,r'''_1,r'''_2} \left\langle \vec{p}' - \frac{\vec{k}}{2}, r'_1, -\vec{p}' - \frac{\vec{k}}{2}, r'_2 \middle| \tilde{T}_{NN,NN}[s = (E^{N}_{\vec{p}'-\vec{k}/2} + E^{N}_{-\vec{p}'-\vec{k}/2})^2 - \vec{k}^2] \middle| \vec{p}''' - \frac{\vec{k}}{2}, r'''_1, -\vec{p}''' - \frac{\vec{k}}{2}, r'''_2 \right\rangle
$$

$$
\times \frac{m^2}{E_{p'''-\vec{k}/2}E_{-p'''-\vec{k}/2}} \frac{1}{2E_p - k - E_{p'''-\vec{k}/2} - E_{-p'''-\vec{k}/2} + i\epsilon} \tilde{V}^{\omega\pi\gamma}_{r'''_1,r'''_2,r''_1,r''_2}(p'',p''',k)
$$

$$
\times \frac{m^2}{E^2_{p'}} \frac{1}{2E_p - 2E_{p'} + i\epsilon} \langle \vec{p}'', r''_1, r''_2 | \tilde{T}_{NN,NN}(s = 4E^{N2}_p) | \vec{p}, r_1, r_2 \rangle. \tag{4}
$$

The initial relative momentum p, final relative momentum p', and photon momentum are fixed by the kinematics. The poles in the propagators of Eq. (4) are treated by a simple subtraction method. Because of the double integral, which requires a very large number of evaluations of $V^{\omega\pi\gamma}$, the calculation of Eq. (4) is extremely time consuming. The other diagrams have similar expressions, and, since they only contain a single momentum integration, are much less elaborate to calculate.

III. RESULTS

The effect of the $\omega\pi\gamma$ diagrams is, similar to that of the Δ-decay diagrams at lower energies, mainly due to interference with the dominant currents. At lower energies this is the nucleonic current, at higher energies both the nucleonic and the Δ-decay current. This implies that the effect on the calculated cross section upon including the $\omega\pi\gamma$ diagrams is linear with their strength: E.g., doubling the $\omega\pi\gamma$ coupling constant gives twice the effect.

In Fig. 2 we present results for the cross section for two geometries from the Triumf experiment at $E_{lab} = 280$ MeV. Here we use the Bonn T matrix in the calculation of the nucleonic current contribution as well as for the evaluation of the $\omega\pi\gamma$ diagrams. Generally speaking the effect of the ω-meson decay process on the cross section is small. At small proton angles its effect is less than 5%; at larger proton angles it tends to be larger but does not exceed 10%. Our results for the Born diagrams (short-dashed lines) are similar, but slightly smaller than those found by the authors of Ref. [18]. This is due to the inclusion of form factors on the NN-meson vertices. These account for the finite size of the nucleon and regularize the momentum integrations in both the single- and double-scattering diagrams. Moreover, including form factors is consistent with using the Bonn T

matrix. With the scales used in Fig. 2, it is difficult to distinguish between the results including $\omega\pi\gamma$ diagrams in the Born approximation (short-dashed lines) and full calculation (long-dashed lines), although at the geometry with large proton angles one can observe a reduction of the $\omega\pi\gamma$ contribution when the corresponding single- and double-scattering diagrams are taken into account. At the point where the effect of the $\omega\pi\gamma$ diagrams is largest ($\theta_\gamma = 80°$), this reduction corresponds to a renormalization of the Born amplitude by a factor 2/3. This is close to the value employed by Jetter and Fearing [18]. Also, here one can argue that the full result can be described by a renormalization of the Born amplitudes. Judging these results we have to bear in mind that the effect of the Δ-decay diagrams is much larger than the $\omega\pi\gamma$ diagrams. Moreover, the Δ-decay diagrams suffer from a relatively large uncertainty due to the not very well determined $N\Delta\gamma$ coupling constant [17].

Results for the analyzing power are presented in Fig. 3. Although the effect of the $\omega\pi\gamma$ diagrams is not large, it affects this observable more at small proton angles than at large proton angles in contrast to the cross section. The shifts
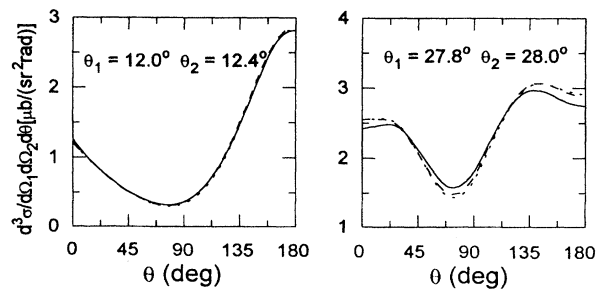
FIG. 2. Cross sections for $E_{lab} = 280$ MeV. The solid line is the result with the nucleon current only, the long-dashed line stands for the full result, and the short-dashed line represents the result with the $\omega\pi\gamma$ diagrams in the Born approximation.
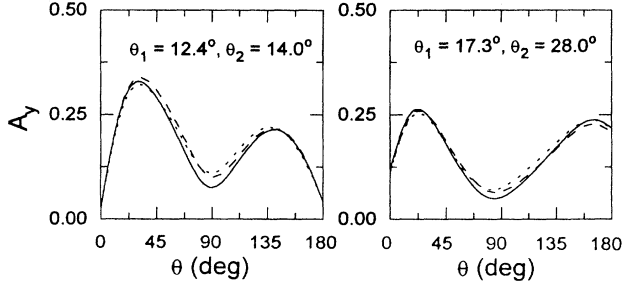
FIG. 3. Same as Fig. 2, but for the analyzing power.

of the analyzing power caused by the $\omega\pi\gamma$ diagrams in both calculations are not in phase, showing that the contribution of the single- and double-scattering diagrams cannot be simulated by a simple renormalization of the Born amplitude. This is not too surprising: The Born amplitude in itself does not generate an analyzing power since it is either purely real or purely imaginary. This in contrast to the single-scattering and rescattering diagrams, which are complex quantities due to the T matrix and they generate an analyzing power on their own.

At $E_{lab} = 550$ MeV the Δ-decay diagrams provide a contribution of the same order as the nucleonic current and we now have to include these diagrams in the calculation of the dominant currents. In the calculation we use a T matrix which includes Δ intermediate states and fits the phase shifts up to 1 GeV. The same T matrix was used in Ref. [17] to which we refer for a more comprehensive treatise on $pp\gamma$ above the pion threshold. In the calculation shown in Fig. 4 the Δ-decay diagrams were calculated with the vector-dominance value of the $N\Delta\gamma$ coupling constant [17]. The
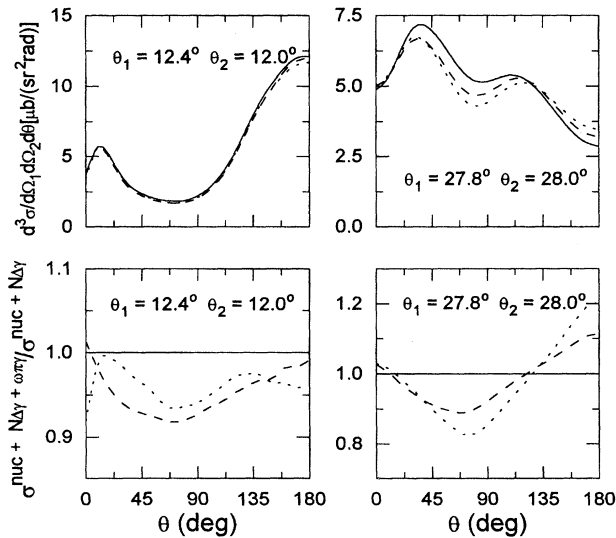
FIG. 4. Same as Fig. 2, but for $E_{lab} = 550$ MeV (upper two panels). In the lower two panels we show the relative cross sections (upper two panels) and relative cross sections (lower two panels). As described in the text, the nucleon current was calculated with a T matrix which includes Δ intermediate states and fits the phase shifts up to 1 GeV.
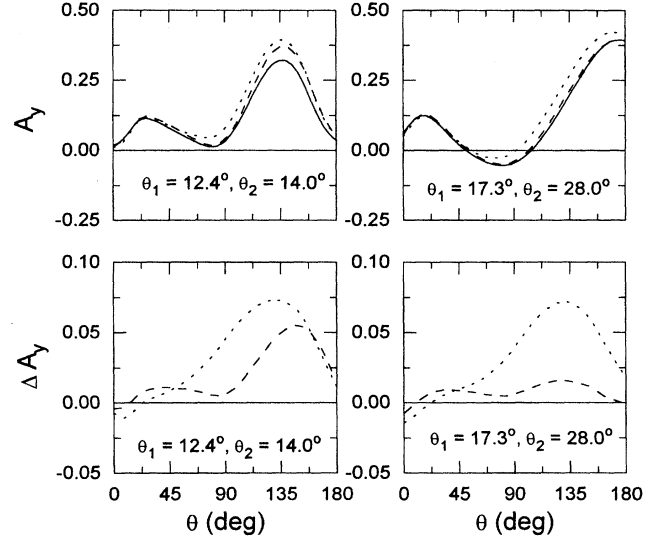
FIG. 5. Same as Fig. 4, but for the analyzing power (upper two panels) and shift in the analyzing power (lower two panels).

counterparts of diagrams 1(b) and 1(c) with a $N\Delta\pi$ vertex are now also included. They provide only a minor contribution.

In Fig. 4 we present cross-section results for the same geometries as discussed previously, but now at $E_{lab} = 550$ MeV. Here, the effect of the $\omega\pi\gamma$ diagrams is larger than at lower energies. For a more detailed comparison of the Born results with the full amplitude we show in the lower panel the effect of the $\omega\pi\gamma$ diagrams relative to the nucleonic and Δ-decay current: $\sigma^{nuc+\Delta N\gamma+\omega\pi\gamma}/\sigma^{nuc+\Delta N\gamma}$. The deviation of this quantity from 1 is a measure of the strength of the $\omega\pi\gamma$ contribution. We observe the same trends as above, but more pronounced. For the geometries at lower proton angles the full result provides a larger shift than the Born result. But again, the differences will be hard to distinguish experimentally. At higher proton angles the single- and double-scattering diagrams reduce the effect of the Born diagrams. Again one can argue that for this geometry the full result can be described by a renormalization of the Born result. This time we find a renormalization factor ~ 0.6 at $\theta_\gamma = 80°$. This is slightly smaller than we found at $E_{lab} = 280$ MeV, which is just the opposite trend as found by Jetter and Fearing [18].

In the results for the analyzing power presented in Fig. 5 we observe notable differences. In the lower panel of Fig. 5 we now plot the shift in the analyzing power upon including the $\omega\pi\gamma$ diagrams ($A^{nuc+\Delta N\gamma+\omega\pi\gamma} - A^{nuc+\Delta N\gamma}$). As long as the shift is small and caused by interference, this quantity is again linear in the strength of the $\omega\pi\gamma$ matrix elements. For both geometries considered we find that the single-scattering and rescattering diagrams tend to reduce the effect of the Born diagrams. At larger proton angles the additional diagrams almost cancel the effect of the Born contribution. We again observe that full calculation cannot be simulated by a simple renormalization of the Born amplitude.

IV. CONCLUSIONS

We investigated the effect of $\omega\pi\gamma$ diagrams on the $pp\gamma$ process. These diagrams are of first order in the photon mo-

mentum. In our approach we include all possible ladder-type diagrams and in this way account for short-range correlations. Since the $\omega\pi\gamma$ diagrams have a similar structure as the diagrams in the NN interaction, one can expect the inclusion of short-range correlations by including the single- and double-scattering diagrams to be important. For most geometries considered where the vector-meson decay process becomes relevant we found that the $\omega\pi\gamma$ single- and double-scattering diagrams reduce considerably the effect of the corresponding Born amplitudes so that the net effect of the vector-meson decay process is much smaller than that estimated from the Born amplitudes alone. At low energies we find an effect which is at most 1/3 of the contribution of the

Δ-decay diagrams, and another contribution of first order in the photon momentum which has been studied recently [16–19]. At higher energies we observed some notable effects. With these results we have to bear in mind though that the uncertainty in the $N\Delta\gamma$-coupling constant creates an uncertainty in the calculated observables which will make it hard to distinguish any of the effects we found.

ACKNOWLEDGMENTS

[1] K. Michaelian et al., Phys. Rev. D **41**, 2689 (1990).

[2] B. v. Przewoski, H.O. Meyer, H. Nann, P.V. Pancella, S.F. Pate, R.E. Pollock, T. Rinckel, M.A. Ross, and F. Sperisen, Phys. Rev. C **45**, 2001 (1991).

[3] R.L. Workman and H.W. Fearing, Phys. Rev. C **34**, 780 (1986); H.W. Fearing, Nucl. Phys. **A463**, 95c (1987).

[4] V. Herrmann and K. Nakayama, Phys. Rev. C **45**, 1450 (1992).

[5] V. Herrmann and K. Nakayama, Phys. Rev. C **46**, 2199 (1992).

[6] V.R. Brown, P.L. Anthony, and J. Franklin, Phys. Rev. C **44**, 2199 (1992).

[7] M. Jetter, H. Freitag, and H.V. von Geramb, Phys. Scr. **48**, 229 (1993).

[8] A. Katsogiannis and K. Amos, Phys. Rev. C **47**, 1376 (1993).

[9] J.A. Eden, D. Pluemper, M.F. Gari, and H. Hebach, Z. Phys. A **347**, 145 (1993).

[10] V. Herrmann and K. Nakayama, Phys. Lett. B **333**, 251 (1990).

[11] V. Herrmann, K. Nakayama, O. Scholten, and H. Arellano, Nucl. Phys. **A582**, 568 (1995).

[12] Y. Ueda, Phys. Rev. **145**, 1214 (1966).

[13] A.N. Kamal and A. Szyjewicz, Nucl. Phys. **A285**, 397 (1977).

[14] A. Szyjewicz and A.N. Kamal, in NN Interactions—1977, AIP Conf. Proc. No. 41, edited by F. Measday, H.W. Fearing, and A. Strathdee (American Institute of Physics, New York, 1978), p. 502; in Few Body Systems and Nuclear Forces I, Proceedings of the Graz meeting, Springer Lecture Notes in Physics Vol. 82, edited by H. Zingl, M. Haftel, and H. Zankel (Springer-Verlag, Berlin, 1978), p. 88.

[15] L. Tiator, H.J. Weber, and D. Drechsel, Nucl. Phys. **A306**, 468 (1978).

[16] F. de Jong, K. Nakayama, V. Herrmann, and O. Scholten, Phys. Lett. B **333**, 1 (1994).

[17] F. de Jong, K. Nakayama, and T.-S.H. Lee, Phys. Rev. C **51**, 2334 (1995).

[18] M. Jetter and H.W. Fearing, Phys. Rev. C **51**, 1666 (1995).

[19] J.A. Eden and M.F. Gari, Ruhr Universitaet Bochum Report No. RUB-MEP-93/94 (nucl-th/9501010), 1995.

[20] B. ter Haar and R. Malfliet, Phys. Rep. **149**, 207 (1987).

[21] S. Krewald, K. Nakayama, and J. Speth, Phys. Rep. **161**, 103 (1988).

[22] R. Machleidt, K. Holinde, and Ch. Elster, Phys. Rep. **149**, 1 (1987).

[23] T.-S.H. Lee, Phys. Rev. Lett. **50**, 1571 (1983); Phys. Rev. C **29**, 195 (1984).

[24] T.-S.H. Lee and A. Matsuyama, Phys. Rev. C **36**, 1459 (1987).

[25] S. Nozawa, B. Blankleider, and T.-S.H. Lee, Nucl. Phys. **A513**, 459 (1990).

[26] H. Garcilazo and E.M. de Goya, Nucl. Phys. **A562**, 521 (1993).